spectra. The remaining portion of the measured broadband spectrum above 1.5-kHz center frequency was closely predicted. Thus the helicopter rotor noise called[6] high-frequency broadband noise is attributed to flow of the blade turbulent boundary layer past the trailing edge. It is adequately predicted by a method developed for calculating such noise from fixed-wing aircraft, applied to local conditions at all radial stations on a rotating blade.

Conclusions

1) Predicted on-axis broadband noise caused by flow of the blade turbulent boundary layer past the trailing edge generally matches the portion of a hovering helicopter rotor's spectrum called high-frequency broadband noise.

2) Noise radiation from nonlifting blades with their shed wakes blown downstream is overestimated near peak amplitude by this method. The same overestimate occurs when predictions by the fixed-wing version of this method are compared with data for nonlifting airfoils. Good agreement occurs at sufficiently higher frequencies for both nonrotating and rotating blades.

References

[1]Fink, M.R., "Airframe Noise Prediction Method," FAA-RD-77-29, March 1977.

[2]Hanson, D.B., "A Study of Subsonic Fan Noise Sources," *Progress in Astronautics and Aeronautics*, Vol. 44, edited by I.R. Schwartz, AIAA, New York, 1976, pp. 209-232.

[3]Ffowcs-Williams, J. and Hall, L.H., "Aerodynamic Sound Generation by Turbulent Flow in the Vicinity of a Scattering Half Plane," *Journal of Fluid Mechanics*, Vol. 40, March 1970, pp. 657-670.

[4]Scheiman, J., Hilton, D.A., and Shivers, J.P., "Acoustical Measurements of the Vortex Noise for a Rotating Blade Operating With and Without Its Shed Wake Blown Downstream," NASA TN D-6364, Aug. 1971.

[5]Schlinker, R.H., "Trailing Edge Noise Measurements With a Directional Microphone," AIAA Paper 77-1269, 4th Aeroacoustics Conference, Atlanta, Ga., Oct. 1977.

[6]Leverton, J.W. and Pollard, J.S., "A Comparison of the Overall and Broadband Noise Characteristics of Full-Scale and Model Helicopter Rotors," *Journal of Sound and Vibration*, Vol. 30, Sept. 1973, pp. 135-152.

Compressibility Effects on Parachute Transient Pressures

Paul C. Klimas*
Sandia Laboratories, Albuquerque, N. Mex.

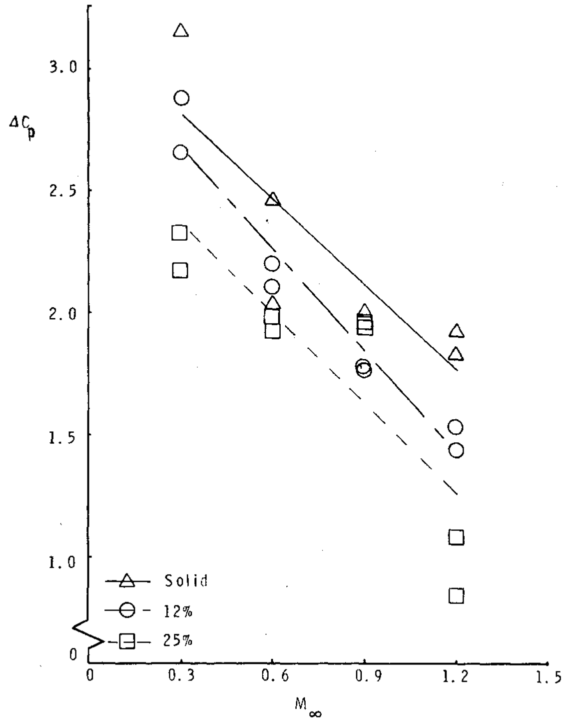

Fig. 1 Transient differential pressure coefficients, $l/r = 0.95$.

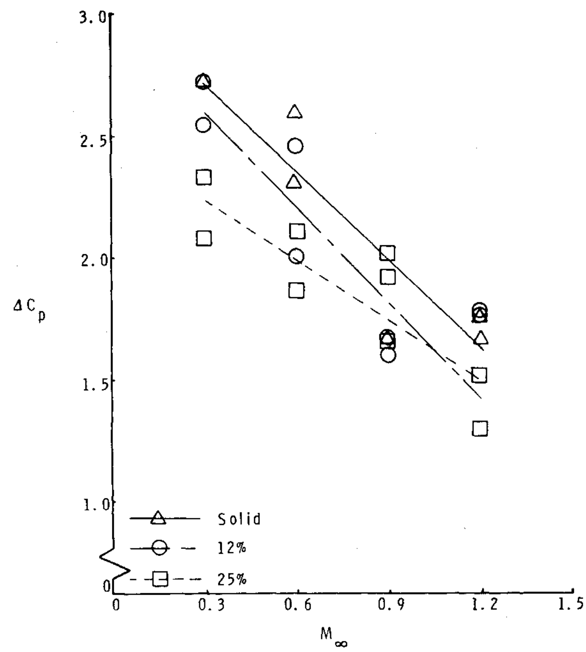

Fig. 2 Transient differential pressure coefficients, $l/r = 0.82$.

Introduction

During inflation of a parachute the peak unsteady differential pressures are greater than corresponding steady values. These transient loadings should ideally be used for canopy structural design, but this is not normally done because the task of analytically describing the unsteady, viscous, often compressible airflow about a flexible, porous structure is a difficult one. Experimentally, the large number of variables (Mach and Reynolds number, canopy geometry, canopy materials, dynamic pressure, mass ratios, etc.) involved in inflation dynamics make it economically unfeasible to run a comprehensive descriptive test program. As a result, most designers account for dynamic effects through design factors determined by trial and error.

Received July 11, 1978.

Index categories: Nonsteady Aerodynamics; Deceleration Systems.

*Member of Technical Staff, Aerodynamics Department 1330. Member AIAA.

Even with the above cited obstacles, two very interesting publications in this subject area have appeared. Melzig and Schmidt[1] measured unsteady pressures on inflating canopies at low subsonic Mach numbers. When expressed in differential pressure coefficient form ($\Delta C_p \equiv (p_{in} - p_{out})/q_\infty$), the maximum unsteady values were often many times the steady values. The multiplier increased as freestream velocity decreased. This qualitative trend was predicted analytically by Eldred and Mikulas[2] through the one-dimensional, unsteady gasdynamical equations. Their formulation showed ΔC_p to be inversely proportional to freestream Mach number. The present work attempts to both expand the available information in this area and isolate the dependence of transient aerodynamics on freestream Mach number. This is done by examining parachutes of three different geometric porosities

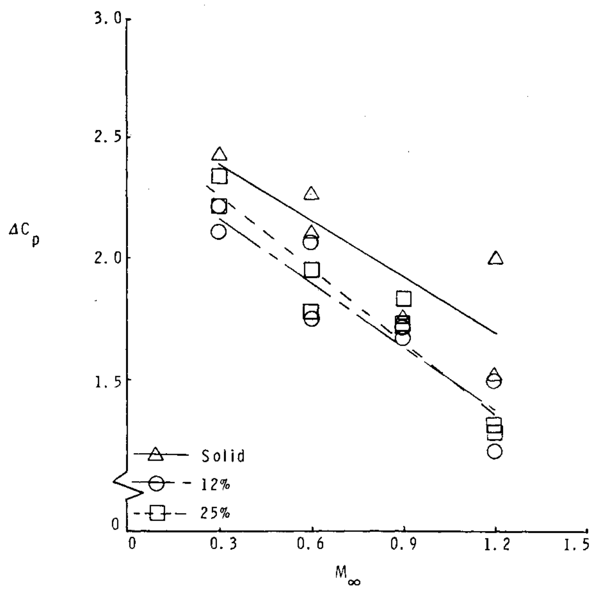

Fig. 3 Transient differential pressure coefficients, $l/r = 0.69$.

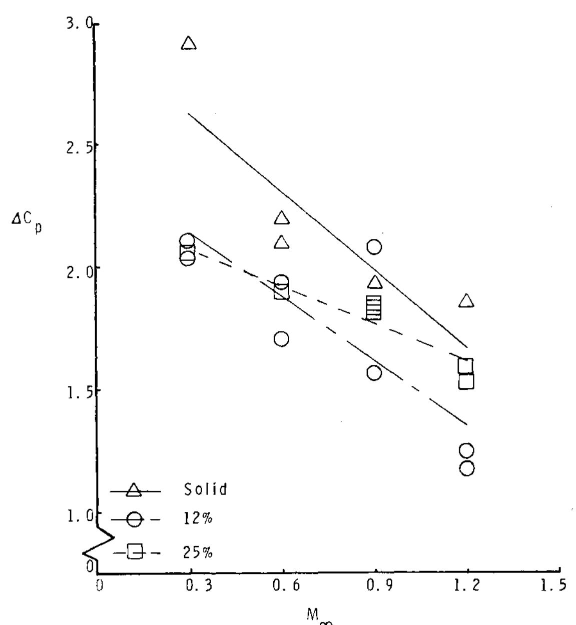

Fig. 4 Transient differential pressure coefficients, $l/r = 0.56$.

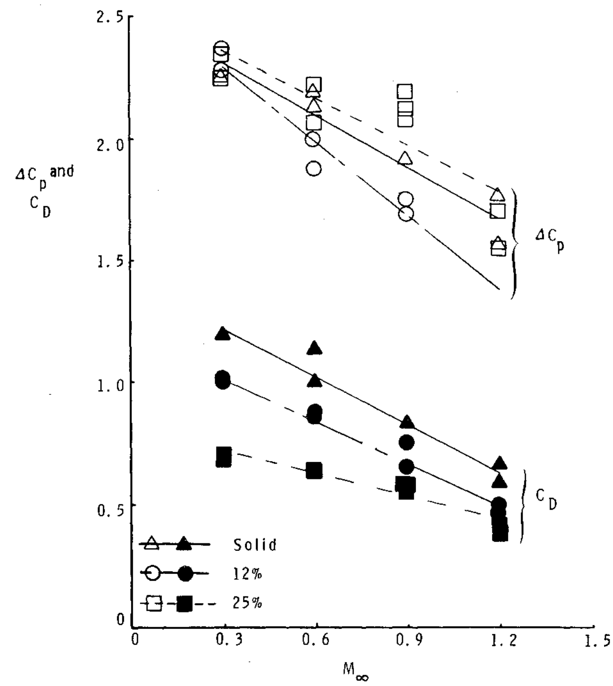

Fig. 5 Transient differential pressure coefficients, $l/r = 0.43$, and transient drag coefficients.

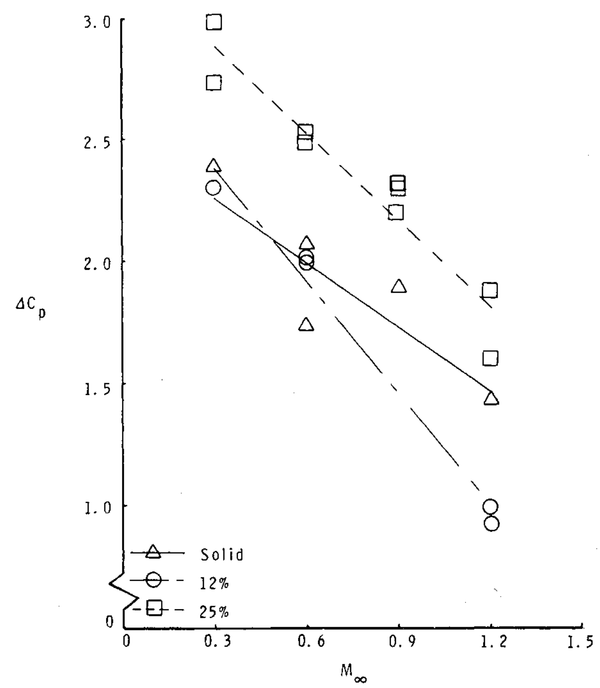

Fig. 6 Transient differential pressure coefficients, $l/r = 0.30$.

(0, 12, and 25%) for $0.3 \leq M_\infty \leq 1.2$ and a constant value of freestream dynamic pressure ($q_\infty = 225$ psf). While far from a complete description, it should provide the basis for more accurate estimates of parachute transient aerodynamic loads.

Experiment

Three nylon parachute models were used. Each had 24 gores, a 3-ft constructed diameter, and 3-ft suspension line lengths. Two were 20-deg conical ribbon canopies of 12% and 25% geometric porosity (λ_g) and the third was a solid flat circular type. Six differential pressure transducers, Kulite Semiconductor Products, Inc., Model #LQH-68-125-250, were evenly distributed circumferentially and sewn to inner radials at equal intervals for $0.95 \geq l/r \geq 0.30$ (r is 18-in radial length, l is local radial location measured from vent center). The models were attached to the aft end of a 32-inch long, 4-inch diameter streamlined body which was cable-mounted along the centerline of the Calspan Corporation 8-ft × 8-ft transonic wind tunnel. The data were obtained in the following manner: 1) a canopy was radially reefed with a 9-inch long nylon line and allowed to stream behind the forebody; 2) the tunnel circuit was either pressurized or evacuated in order to provide a constant 225 psf q_∞ at M_∞'s of 0.3, 0.6, 0.9, and 1.2; 3) when the desired M_∞ was reached, an electrically actuated explosive reefing line cutter was fired and the output from the six transducers was subsequently recorded on magnetic tape. A total of 23 runs on the three canopies at the four M_∞'s were made.

Results and Conclusions

Maximum values of ΔC_p are given in Figs. 1-6 for various radial locations. Also given are first-order least-squares fits for these points and the maximum drag coefficients for each run (Fig. 5). Linear fits were chosen because of the relatively small amount of data.

The salient observation is that $\Delta C_{p_{max}}$ is a reasonably strong and monotonically decreasing function of M_∞. In terms of magnitudes, the essentially incompressible flow ($0.05 \leq M_\infty \leq 0.15$) results of Ref. 1 provide a basis for partial comparison for the solid and 12% λ_g canopies. The Ref. 1 ribbon parachute (15% λ_g) exhibited peak pressures which were numerically similar to the $M_\infty = 0$ predictions from the 12% λ_g least-squares line. This was not the case for the solid flat circulars. The Ref. 1 values ran 65 to 95% higher than present $M_\infty = 0$ linear extrapolations. The qualitative trends associated with changes in porosity as noted for static conditions (Ref. 3) appear to also apply here. The highest skirt region pressures are felt by the lowest porosity canopy while the greatest vent area ΔC_p's are generated by the most porous model. Maximum drag coefficients are quite accurately represented by linear fits and, as expected, show an M_∞ dependence which is similar to that of the pressures.

No steady state pressure results are given. Large tunnel blockages due to full open canopies changed tunnel conditions from the pre-disreef values. These changes became larger as M_∞ increased and represented a 30-35% decrease in both M_∞ and q_∞ at the nominal $M_\infty = 1.2$ setting. This eliminated all meaningful bases for comparison between dynamic and steady measurements. The "steady" (as tunnel conditions were slowly changing) drag coefficients as given by the tunnel data system were 0.66, 0.60, and 0.48, all ± 0.06, for the three canopies in order of increasing porosity. Those values are averages of approximately 300 data points and fall into the range $0.25 < M_\infty < 0.85$.

References

[1] Melzig, H. D. and Schmidt, P. K., *Pressure Distribution During Parachute Opening, Phase I, Infinite Mass Opening Case,* Technical Report AFFDL-TR-66-10, March 1966.

[2] Eldred, C. H. and Mikulas, M. M. Jr., "Transient Aerodynamic Pressures During Unsteady Parachute Processes," AIAA Paper 70-1175, Dayton, Ohio, Sept. 1970.

[3] Pepper, W. B. and Reed, J. F., "Parametric Study of Parachute Pressure Distribution by Wind Tunnel Testing," *Journal of Aircraft,* Vol. 10, Nov. 1976, pp. 895-900.